Elastic model of supercoiling

(DNA/superhelicity/elasticity)

CRAIG J. BENHAM*

Division of Biology, California Institute of Technology, Pasadena, California 91125

ABSTRACT   An elastic model for the supercoiling of duplex DNA is developed. The simplest assumptions regarding the elastic properties of double-helical DNA (homogeneous, isotropic, of circular cross section, and remaining straight when unstressed) will generate two orders of superhelicity when stressed. Recent experimental results [Brady, G. W., Fein, D. B. & Brumberger, H. (1976) *Nature* 264, 231–234] suggest that in supercoiled DNA molecules there are regions where two distinct orders of supercoiling arise, as predicted by this model.

The role of elasticity in supercoiling of DNA is investigated by ascribing to the double helix the properties of a homogeneous, isotropic elastic rod. The unstressed molecule has helical twist of one turn per ten base pairs. As an elastic object, this idealized molecule resists deviations from straightness and from its unstressed twist with certain bending and torsional stiffnesses.

Linear DNA with free ends may deform so as to relieve internal stresses. In its covalently closed, circular form, however, the molecule experiences torsional and bending stresses which cannot be relieved without breaking one of the strands (nicking) (2). Stresses may be varied by external constraints such as dye intercalation (3).

If the stresses involved are not too great, the molecule may respond as a whole by deforming into an equilibrium shape. (In this paper "equilibrium" refers to elastic, *not* thermodynamic, equilibrium.) However, if the stresses are sufficiently large, they may cause local denaturation (4, 5). Disruption of the double helix alters or destroys the elastic properties of the denatured regions, thereby permitting the relief of excess torsional stress through winding or unwinding. In this case, the regions of double helix between adjacent denatured portions deform into equilibrium shapes in response to the stresses imposed on them.

The equilibrium shapes possible in these situations may be found from Kirchhoff's theory of linear elastic rods (6). This allows explicit calculation of shapes as desired. It also permits a suggestive visualization of the possible shapes through a rigorous analogy between deforming rods and spinning tops.

In summary, it is found that three equilibrium shapes are possible. If the stresses are sufficiently small, a section of double helix may remain straight (neglecting kinetic effects). If the straight shape is not possible, then the double helical sections of the idealized molecule (which may be the whole molecule) will deform either into a (super) helix (a first order supercoil) or into a shape having two orders of superhelicity. Deformation into a (super) helix requires very precise conditions on the imposed loads, and is thereby unlikely to occur in practice.

Recent experimental evidence (1) suggests that in supercoiled DNA are found regions exhibiting two orders of superhelicity, as predicted by the theory. This suggests that the elastic model may be adequate to predict supercoiling in DNA.

* Present address: Mathematics Department, Lawrence University, Appleton, WI 54911.

ELASTIC THEORY

Two cases are considered here—elastic deformations of closed rings and of linear rods. Only undenatured regions of double helix are modeled as elastic, which may be either the whole ring or linear sections of the ring. However, the theory of deformation of a rod with forces and torques on its ends includes the case of an elastic ring. That is, the ring at equilibrium may be cut at one cross section, and a system of forces applied to the ends created. If this system is equal to that by which, in the original closed ring, each side of this cross section acts on the other, then the equilibrium shapes of rod and ring will be identical.

In this model the stresses experienced by the elastic rod are treated as follows: Consider the cross section at distance s_o from one end ($s = 0$). That side of the cross section where $s < s_o$ acts on the other side ($s > s_o$) with a system of forces that is resolvable (7, 8) into a force $N(s_o)$ and a torque $M(s_o)$. Doing this at each cross section gives (vector-valued) functions $N(s)$, $M(s)$ describing the stresses in the rod. (Note that if one begins at the opposite end of the rod the force and torque found change their sign. The two sides of any cross section act on each other with equal and opposite systems of forces.)

Some choices of $N(s)$ and $M(s)$ will cause acceleration of the rod. Others cause rotation, while still others give rise to dynamic deformations. Most choices will yield a combination of all three motions. Those systems $N(s)$, $M(s)$ that occur when the rod is in an equilibrium shape must satisfy special criteria, called the equations of equilibrium (8, 9):

$$dN/ds + \kappa(s) \times N = 0 \qquad [1a]$$

$$dM/ds + \kappa(s) \times M + k(s) \times N = 0. \qquad [1b]$$

Here $\kappa(s)$ is the curvature of the rod and $k(s)$ is the unit tangent vector to the rod (in the direction of increasing s), both evaluated at each distance s.

Eqs. 1a and 1b above are two first-order ordinary differential equations describing those systems $N(s)$ and $M(s)$ that arise at equilibrium. To determine a unique solution one must specify the force and torque that arise at a single cross section, taken here to be $M(o)$ and $N(o)$, the torque and force on one end. For each such choice there is a single equilibrium system $M(s)$, $N(s)$ having those values for $M(o)$ and $N(o)$.

Physically, this means that one may specify the force and torque imposed on one end of the rod at will. The solution of Eqs. 1a and 1b above uniquely determine the force $N(s)$ and the torque $M(s)$ across every other cross section if the rod is in equilibrium under the specified load. In particular, the force and torque that must be imposed on the opposite end of the rod for equilibrium to occur are specified.

To describe the shape of the rod we introduce Euler's angles. Then linear elastic laws relating deformations to stresses are used to find three well-known differential equations, one for
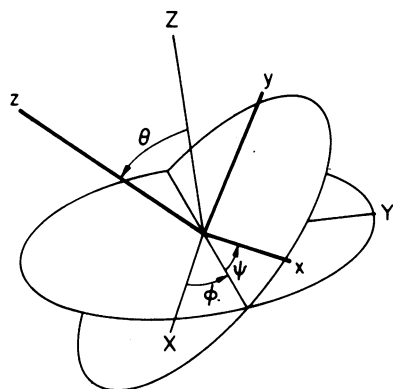
FIG. 1.   The Euler angles θ, ϕ, ψ relating the fixed space axes X, Y, Z to the moving body axes x, y, z.

each Euler angle. Solution of these gives the equilibrium shape of the rod under the given loads.

At *each* distance s along the rod a system of local, body coordinates $x(s)$, $y(s)$, $z(s)$ is chosen so that the $z(s)$ axis points tangent to the rod in the direction of increasing s while the $x(s)$ and $y(s)$ axes are principal axes of the cross section. A reference set of space axes X, Y, Z is fixed. To compare the orientations of the body and space coordinate systems, Euler's angles θ, ϕ, ψ, are used, as in Fig. 1. Rotation through these angles brings the space axes into alignment with the body axes. For a deformed rod the orientation of the local body axes changes as the rod is transversed, so Euler's angles vary with distance, $\phi = \phi(s)$, $\psi = \psi(s)$, $\theta = \theta(s)$.

Two cross sections of the rod separated by an infinitesimal distance Δs have their body axes infinitesimally rotated by a vector $\Delta\Phi$. The vector curvature of the rod at any point s is

$$\kappa(s) = \lim_{\Delta s \to 0} \frac{\Delta\Phi}{\theta s} = \frac{d\Phi}{ds} \qquad [2]$$

which has components $[\kappa_x(s), \kappa_y(s), \tau(s)] = \kappa(s)$ in the $x(s)$, $y(s)$, $z(s)$ directions. Here $\kappa_x(s)$, $\kappa_y(s)$ are the curvatures of the rod in the principal directions at distance s, while $\tau(s)$ is the rate of twist (i.e., rotation about the tangent). These may be expressed in terms of Euler's angles as

$$\kappa_x = \dot\phi \sin \theta \sin \psi + \dot\theta \cos \psi, \qquad [3a]$$

$$\kappa_y = \dot\phi \sin \theta \cos \psi - \dot\theta \sin \psi, \qquad [3b]$$

$$\tau = \dot\phi \cos \theta + \dot\psi. \qquad [3c]$$

where the dot stands for differentiation with respect to s in the local body coordinates.

The elastic laws relating deformations to loads are assumed to be linear:

$$M_x(s) = A\kappa_x(s), \; M_y(s) = B\kappa_y(s), \; M_z(s) = C\tau (s). \qquad [4]$$

The constants A,B are the bending stiffnesses in the x,y directions, while the torsional stiffness is C. If the rod bends as easily in the x and the y directions, then $A = B$ and the rod is symmetric. In this case one can show that the rate of twist $\tau(s)$ in the rod deformed to equilibrium is a constant, $\tau(s) = \tau_o$.

From Eq. 1a it follows that the vectors $N(s)$ which occur at equilibrium are constant in magnitude, $|N| = N$, and direction in space at every cross section. The fixed space Z axis is chosen to point in the direction of N.

From Eqs. 1b, 3, and 4 and the condition of symmetry ($A = B$) one can derive (using a Lagrangian analysis) three differ-

ential equations for the Euler angles of a symmetric rod at equilibrium:

$$\dot\phi = \frac{p_\phi - p_\psi \cos \theta}{A \sin^2 \theta} \qquad [5]$$

$$\dot\psi = \frac{p_\psi}{C} - \frac{p_\phi - p_\psi \cos \theta}{A \sin^2 \theta}\cos \theta \qquad [6]$$

$$N \cos \theta + \frac{(p_\phi - p_\psi \cos \theta)^2}{2A \sin^2 \theta} + \frac{A\dot\theta^2}{2} = \left(E - \frac{p_\psi{}^2}{2C}\right) = \overline{E}. \qquad [7]$$

Here p_ϕ, p_ψ are the generalized momenta conjugate to the generalized coordinates ϕ, ψ. They are constants determinable from initial conditions, as is $\overline{E}$.

Letting $u = \cos \theta$ the last equation becomes

$$\dot u^2 = f(u) = \frac{2}{A}(\overline{E} - Nu)(1 - u^2) - \frac{(p_\phi - p_\psi u)^2}{A^2}. \qquad [8]$$

The function $f(u)$ has three real roots $-1 \leq u_1 \leq u_2 \leq +1 \leq u_3$. The physical limits of u are $u_1 \leq u \leq u_2$ because only here is $f(u) \geq 0$ so that $\dot u$ is not imaginary. Solution of these equations gives the equilibrium shape of the rod through Eq. 3. A useful visualization of the possible equilibrium shapes has been found by Kirchhoff.

THE KINETIC ANALOGY AND EQUILIBRIUM SHAPES

A formally precise analogy, known as Kirchhoff's theorem (6), exists between a rod at equilibrium under the influence of forces applied to its ends and a top spinning about a fixed point. The equations describing these two situations are identical, so any solution of either problem also solves its analogue. If the rod has symmetry, the analogous top will also be symmetric, with its center of mass and fixed point lying on a principal axis. In this situation an exact solution to the equations for the motion of a top has been found (10, 11). By Kirchhoff's theorem, this solves the symmetric rod.

To make the analogy precise, consider a symmetric spinning top. At its fixed point it has three principal (body) axes which move with it. The body z-axis passes through the fixed point and the center of mass. Fixed space axes are chosen so that the space Z axis points opposite to Mg, the force of gravity on the top. The relationship of body axes to space axes is given by Euler's angles, as before. In particular, θ is the angle between the body z axis and the vertical. As the top spins, the body axes are carried along so that Euler's angles change with time.

Kirchhoff (6) noted that the differential equations describing the motion of the top in terms of Euler's angles are formally identical with those for the equilibrium shape of a rod. With the appropriate interpretation of the variables given in Table 1, Eqs. 5, 6, and 8 are found to apply to both cases.

An easy way to visualize the Kirchhoff analogy is to imagine that one traverses the rod at unit speed. As one travels, the rod's body axes appear to rotate relative to the space axes. This motion is identical to the motion of the axes embedded in a spinning top whose moments of inertia, mass, etc., are given by the correspondence shown in Table 1.

In 1811, Lagrange (10) showed that the equations of the symmetric top are integrable. The solution involves elliptic functions and may be found, for instance, in ref 11. By Kirchhoff's theorem, this gives a solution to the analogous problem of a symmetric rod subjected to forces and couples on its ends.

In general, three types of motion of a symmetric top are possible. First, it may spin about its z-axis while remaining vertical ($\theta = 0$). Second, it may precess uniformly at a constant

Table 1. Analogous variables for rod and top

Variable	Rod	Top
s	Distance	Time t
A, B, C	Stiffnesses	(I_x, I_y, I_z) Moments of inertia
κ	Curvature	ω, Angular velocity
$(\kappa_x, \kappa_y, \tau)$	Curvature components	$(\omega_x, \omega_y, \omega_z)$ Components of ω
$-N$	(Negative of) stress resultant (constant at all s)	mg, force of gravity (Constant at all t)
p_ϕ, p_ψ	Conjugate momenta	Conjugate momenta
M	Torque	Angular momentum L

angle $\theta \neq 0$. Finally, as it precesses it may also nutate (bob between two values of θ). These correspond to the analogous rod remaining straight or deforming into a helix of pitch angle $90°$ $- \theta$ (a first-order supercoil) or deforming into two orders of supercoils. These shapes may be visualized as in Fig. 2 by plotting on a unit sphere the tangent direction of the rod. If the rod remains straight, this direction does not change. Deformation into a helix causes the tangent to describe a circle as in Fig. 2B. A rod deformed into two orders of supercoils (a top that precesses and nutates) gives rise to motions of its tangent such as those shown in Fig. 2 C and D.

For a rod of length l at equilibrium, on one end of which is imposed a force N (0) and a torque M (0) that are coaxial, the straight conformation is always an equilibrium shape (12). However, only when

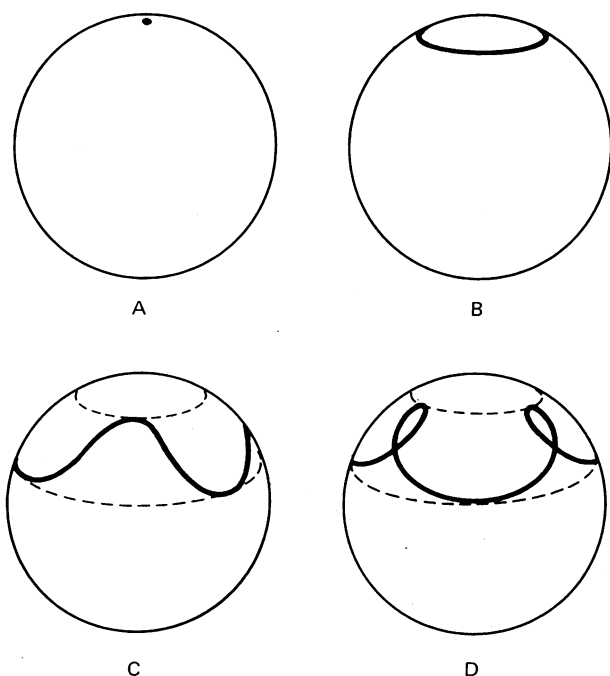$$\frac{\pi^2}{l^2} \geq \frac{M^2}{4A^2} + \frac{N}{A} \qquad [9]$$

C   D

FIG. 2. The motion of the body z-axis plotted on a unit sphere for various deformed shapes. (A) The rod remains straight. (B) The motion that occurs when the rod deforms into the helix. The analogous top precesses uniformly. (C and D) Two possible second-order supercoils, which correspond to a top both precessing and nutating. In (C) the Euler angle ϕ increases uniformly while in (D) it changes sign in each nutation cycle.
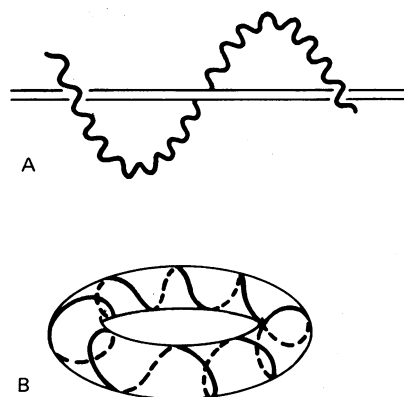

FIG. 3. Possible shapes of an elastic molecule. The line plotted is the axis of the double helix. (A) A linear section deforms into two orders of supercoils, as could occur through dye intercalation. (B) A toroidal superhelix, one possible shape for a covalently closed ring.

is the straight shape stable. For values of M, N that do not satisfy Eq. 9 the stable shape will have either one or two orders of supercoiling.

Suppose now that the applied torque $M(0)$ is tangential, $M(0)$ $= M_z k(0)$, and the angle between $M(0)$ and $N(0)$ is θ_o. Then $\cos \theta_o = u_o = u_2 \leq 1$ gives the upper limit of the physical range of the variable u. The circle $u = u_2 = u_o$ is the upper bound on the analogous nutation in Fig. 2 C and D. The other two roots of Eq. 8 satisfy

$$u_o - u_j = \frac{2NA}{p_\psi^2}(1 - u_j^2).$$

The rod forms a helix precisely when $u_1 = u_2 = u_o$. From the above equation this occurs when $u_1 = u_2 = \pm 1$ so the rod remains straight. Therefore, when the initial torque is tangential and the rod is not straight, its equilibrium shape must have two orders of supercoiling (Fig. 3A), called here the precessional and nutational orders.

If the straight conformation is not stable and the initial torque is not tangential, then a pure helix can arise of pitch angle $90°$ $- \theta_o$ and either of two possible radii. The analogous top undergoes either a slow or a fast precession, which may be shown to be in the same direction as the twist τ (13).

Deformation into a helix (analogous to uniform precession) occurs only in the exceptional situation where the two smallest roots of $f(u)$ in Eq. 8 coincide, $u_1 = u_2$. In general, θ (and hence u and the pitch angle $90° - \theta$) will vary between the limits θ_1 and θ_2 where $\dot{\theta} = 0$. The precession angle ϕ satisfies Eq. 5. If the numerator of this equation is never zero within the physical range $u_1 \leq u \leq u_2$, then ϕ always moves in one direction, as in Fig. 2C. If $u_1 < p_\phi/p_\psi < u_2$, then ϕ changes sign whenever $u = p_\phi/p_\psi$ (Fig. 2D). If $p_\phi/p_\psi = u_2$ (as happens when the applied torque is tangential), there is a cusp of the motion on the upper circle. As the tangential component M_z of the applied torque increases (other things remaining equal) the two circles $u = u_1$ and $u = u_2$ move closer together. The nutational supercoils become inconspicuous, so the shape approximates a helix of radius

$$r = \frac{C\tau}{2N} = \frac{C\tau u_o}{2\bar{E}}. \qquad [10]$$

APPLICATIONS TO SUPERCOILING

In this section the results developed for the equilibrium shapes of thin elastic rods subject to stresses are applied to supercoiling

of DNA. First, a molecular origin for the stresses is proposed. Then the equilibrium shapes possible under given stresses are described using the results of the last section. Local denaturation (and possible kinking) are modeled as the breakdown of the elastic laws under high stresses. In these cases the elastic analysis can be applied only to regions of double helix. In this way, the theory includes deformation of linear, rodlike elastic pieces of double helix as well as of complete, closed rings.

In its covalently closed, circular form a molecule of duplex DNA has linking number Lk (14, 15), an integer measuring the number of times one strand links through the other. This Lk cannot change unless a strand is broken (nicked), so it is fixed when the strands close. If the helix is wound without constraint, before closing it will have equilibrium twist $T = T_o$. When covalently closed into a circle its linking number is $Lk = T = T_o$.

It may happen that the helix is under- or over-twisted at the time of covalent closure, $T \neq T_o$. (Note that the total twist T is related to τ by $2\pi(T - T_o) = \int \tau ds$.) The twist also may be changed by external constraints (such as dye intercalation) after closure. The deficiency or excess that arises due to either of these causes is expressed as the writhing number Wr (14, 15) of the molecule. Thus,

$$Lk = Wr + T. \qquad [11]$$

This quantity Wr depends only on the shape of the *axis* of the double helix. As the molecule bends, Wr may vary continuously (14, 15). However, Lk is a topological invariant, which cannot change unless the molecule is nicked. Thus, changes in shape will cause compensating changes in the total twist T so as to leave Lk invariant.

In covalently closed molecules elastic stresses may arise which cannot be relieved without changing Lk. As an example, a molecule that is underwound at the time of covalent closure will experience elastic stresses trying to twist it up to the equilibrium value T_o. It can twist only at the expense of changing Wr, that is, of bending (Eq. 11). But bending causes elastic restoring stresses also. Thus, the molecule settles into an equilibrium conformation balancing its torsional and bending stresses. Precisely how the stresses are partitioned will depend upon the ratio A/C of elastic constants.

Changing the linking number Lk causes compensating changes in T and Wr (and hence in equilibrium shape) in accordance with Eq. 11. Using gel electrophoresis, molecules of different Lk may be separated (16, 17).

The local twist τ may be varied by external constraints such as dye intercalation. It is known that the intercalation of ethidium bromide untwists (18) the site of binding by 26°. The regions between binding sites, as elastic objects, will resist a compensating twisting. Thus, dye binding causes changes *both* in the total twist T *and* in the writhing number Wr (i.e., the shape of the molecule).

In our model the untwisting caused by dye intercalation corresponds to the case of *tangential* applied torque on the rod. The elastic theory makes two predictions in this case. First, an elastic rod deforming under a tangential torque always exhibits two orders of supercoiling (see Fig. 3A). Second, as the torque is increased (i.e., as more dye is bound), this shape approximates a helix.

One can also predict shapes of closed rings (in the absence of local denaturation). A necessary (but *not* sufficient) condition for ring closure is that the curve of tangents of Fig. 2 be closed. If this curve also crosses every great circle, then there is a closed-ring shape with this curve as its curve of tangents (19). One possible shape for a closed molecule is a toroidal helix, as

in Fig. 3B. This arises when $u_1 = -u_2$ and there are m supercoils in one trip around the ring.

Sufficiently large elastic stresses may cause local denaturation (and perhaps also kinking) of the molecule (4, 5). The disruption of the double helix alters or destroys the elastic properties of the regions involved. The denatured regions could take up excessive (or deficient) twist (3) by a disorganized winding, thereby relieving (at least partially) the excess stresses on the double-helical portions. In the simplest case there could be a threshold twist rate τ beyond which all further stresses go into denaturation.

DISCUSSION AND CONCLUSIONS

The elastic model of supercoiling presented rests upon the assumption that double-helical DNA has the elastic properties of a homogeneous, isotropic, symmetrical rod. The theory makes qualitative predictions of equilibrium shapes involving two orders of supercoiling. Recent experimental evidence (1) suggests that native closed, circular PM2 viral DNA exhibits regions with two orders of supercoiling, as would arise from the above elastic properties.

Before quantitative predictions of shape are possible, the bending stiffness A and torsional stiffness C of DNA must be evaluated. An experimental determination of an effective bending stiffness of linear DNA has been made from sedimentation data (20). It may be possible to determine the torsional stiffness C from existing data on the free energy of supercoiling (16, 21). The present theory also suggests methods for evaluating C either from Eq. 9 for the onset of supercoiling or from Eq. 10 for the shape at large twist (assuming no denaturation).

This model assumes the simplest elastic properties. The symmetry condition is that the bending stiffnesses in the two principal directions are equal, $A = B$. This may not be strictly correct on the scale of the double helix. Nevertheless, it is a reasonable approximation if the bends involved in supercoiling are spread over several turns of the double helix (as is suggested by the x-ray data of ref. 1). The present model is being refined to include possible asymmetries, as well as shear and deformation of the cross section.

An important assumption implicit in the present theory is the absence of crossing forces. These arise when the molecule tries to cross itself in getting to its equilibrium shape. The molecule is barred from equilibrium, and settles instead into a metastable state. In a kinetic environment it may eventually reach equilibrium in spite of crossing forces.

The ionic and solvent influences on the DNA could be subsumed into the effective elastic properties, but kinetic and statistical effects must be investigated separately. Landau and Lifshitz (22) and others have developed the statistics of long-chain, linear elastic polymers. However, unconstrained linear molecules can relieve stresses by bending and twisting freely. The situation is different for a covalently closed molecule, for now the molecule cannot bend and twist to relieve stresses. (Also the entropic contribution is smaller due to the identified ends.) It is constrained to shapes that satisfy Eq. 11. The effects of closure (through the linking number Lk) can impose a highly organized global structure on the molecule.

Finally, a careful analysis of the role of local denaturation in supercoiling is needed.

The conclusions of the present analysis when taken in conjunction with the experimental results of Brady *et al.* (1) suggest that elastic properties can account for supercoiling, and that studies of supercoiling, in turn, may permit determination of the elastic constants of DNA.

Biophysics: Benham

Proc. Natl. Acad. Sci. USA 74 (1977) 2401

1. Brady, G. W., Fein, D. B. & Brumberger, H. (1976) *Nature* **264,** 231–234.
2. Bauer, W. & Vinograd, J. (1968) *J. Mol. Biol.* **33,** 141–171.
3. Wang, J. C. (1969) *J. Mol. Biol.* **43,** 25–39.
4. Dean, W. W. & Lebowitz, J. (1971) *Nature New Biol.* **231,** 5–8.
5. Beerman, T. A. & Lebowitz, J. (1973) *J. Mol. Biol.* **79,** 451–470.
6. Kirchhoff, G. (1859) *J. F. Math (Crelle)* **50,** 285–313.
7. Symon, K. R. (1960) *Mechanics* (Addison-Wesley, Reading, MA), 2nd ed., pp. 228–229, 461–468.
8. Love, A. E. H. (1927) *A Treatise on the Mathematical Theory of Elasticity* (Dover, New York), 4th ed.
9. Landau, L. D. & Lifshitz, E. M. (1959) *Theory of Elasticity* (Addison-Wesley, Reading, MA), pp. 79–85.
10. Lagrange, J. L. (1811–1815) *Mecanique Analytique,* revised ed.
11. MacMillan, W. D. (1936) *Dynamics of Rigid Bodies* (Dover, New York), pp. 216–256.
12. Greenhill, A. G. (1883) *J. Inst. Mech. Eng. London,* 182–225.
13. Hadamard, J. (1895) *Bull. Sci. Math., 2 Ser.* **19,** 228–230.
14. Fuller, F. B. (1971) *Proc. Natl. Acad. Sci. USA* **68,** 815–819.
15. Crick, F. H. C. (1976) *Proc. Natl. Acad. Sci. USA* **73,** 2639–2643.
16. Depew, R. E. & Wang, J C. (1975) *Proc. Natl. Acad. Sci. USA* **72,** 4275–4279.
17. Bauer, W. & Vinograd, J. (1974) in *Basic Principles in Nucleic Acid Chemistry,* ed. T'so, P. (Academic Press, New York), pp. 265–303.
18. Sobell, H. M., Tsai, C., Gilbert, S., Jain, S. & Sakore, T. D. (1976) *Proc. Natl. Acad. Sci. USA* **73,** 3068–3072.
19. Vigodsky, M. (1945) *Math. Sbornik* **16,** 73–80.
20. Gray, H. B. & Hearst, J. (1968) *J. Mol. Biol.* **35,** 111–129.
21. Pulleyblank, D. E., Shure, M., Tang, D., Vinograd, J. & Vosberg, H. P. (1975) *Proc. Natl. Acad. Sci. USA* **72,** 4280–4284.
22. Landau, L. D. & Lifshitz, E. M. (1958) *Statistical Physics* (Addison-Wesley, Reading, MA), pp. 487–482.